

There are several factors which will often minimize the effects of the standing waves produced by reflections. This analysis was conducted for the uncontrolled environment, which is based upon a 30 minute averaging time. It is highly unlikely that an individual would remain fixed in one location for that period of time. As can be seen in Figures D-3 and D-4, a small movement by the individual can materially reduce the instantaneous level of exposure. Furthermore if the exposure were to be averaged over the space actually occupied by the individual over the 30 minute period, it would almost certainly be importantly less than the maximum shown in this analysis.

Also, as discussed elsewhere in this filing, the general public is seldom able to gain access to antenna site locations. Thus, in most cases, the limits applicable to the controlled environment should be used, which will substantially reduce the required separation distance to meet the ANSI standard. Finally, many installations involve transmitters which are of substantially lower power than used in this analysis, and the duty cycle of those transmitters is less than 100% further reducing the average exposure. On the basis of these and other factors, and the analysis presented herein, it is believed that reflections are not likely to normally have a significant impact upon the exposure level experienced by individuals in the vicinity of land mobile base station sites.

## **CONCLUSION**

Computations have been made to determine the required distance from a typical high band 3 dB antenna radiating 300 watts that is necessary to meet the "Uncontrolled Environment" MPE of ANSI C95.1-1992. The antenna is mounted in the presence of reflectors that produce standing waves of both E and H. The horizontal distance from the antenna to the point where the MPE is met is less than 3 meters.

## ELECTROMAGNETIC ENERGY EXPOSURE OF THE USERS OF PORTABLE CELLULAR TELEPHONES

Q. Balzano - O. Garay - T. Manning

### I. Introduction

Recently, there has been speculation that the use of portable cellular telephones may stimulate the growth of human brain tumors in the region of the head in proximity to the antenna [1]. This speculation has triggered some lawsuits and the advent of a variety of devices, called antenna shields, whose claim is to substantially decrease the exposure of the users of cellular telephones to the RF electromagnetic energy from the antenna without excessively degrading the coverage performance of the telephone .

This paper does not address in detail the issue of brain carcinogenesis of RF electromagnetic energy; it deals essentially with the dosimetric aspects of the exposure of users of cellular telephones. In addition it presents an experimental analysis of the performance of some antenna shields currently available on the market.

### II. Methodology and Measurement Apparatus

#### a. Significant Exposure Parameters

The exposure of users of cellular telephones can be quantified in terms of incident electric and magnetic fields or the Specific Absorption Rate (SAR) which measures the rate at which total electromagnetic energy is absorbed by lossy dielectric media, with non-magnetic dissipative properties [2]. Previous research showed that the incident electric field is poorly correlated with the electromagnetic energy that actually penetrates deeply into the tissue [3]. With present knowledge, brain tissue absorbs RF electromagnetic energy essentially through Joule heating associated with rotational motion collisions of large and small polar biomolecules and by ohmic losses of freely moving ions in the cellular fluids [4].

Recently some traces of biomagnetite have been found in the human brain [5], but their biological import in terms of RF electromagnetic energy absorption in the frequency band of cellular telephones (824 - 849 MHz) remains unclear. In the absence of known relevant magnetic absorption phenomena of the organs residing in the human head, the obvious and best choice for characterizing the exposure of the user of cellular telephones is the Specific Absorption Rate or SAR.

As will be shown in the following sections, evaluation of the magnetic field in the close vicinity of the cellular telephone is an excellent diagnostic tool to analyze the RF currents on the cellular telephone antenna and radio case. Since, close to RF sources, the SAR patterns are well correlated with the near magnetic field distribution, it is important during the design phase of a cellular telephone to establish that no undesired RF current bunching effects, due to stray phenomena, are accumulating at locations close to the head of the user.

The electric and magnetic field probes used in the measurements of SAR and near magnetic field have been already described in the literature [6] and [7]. The measurement apparatus and the calibration of the probes will be discussed in the next sections. The temperature increase method to measure SAR [8] cannot be used in conjunction with portable cellular telephones because of the low RF power emitted by these devices: 0.6W. The temperature increase method has been used to calibrate the SAR-sensing probes.

b. Phantom Model

The phantom model, the simulated human head to be used in the SAR measurements, has been selected with several criteria in mind. The SAR tests are not aimed to determine with great accuracy the RF absorption pattern in a specific anatomy or a set of specific anatomies. The tests are aimed to measure the highest peak SAR value that could happen in the head of a user. The SAR tests were set up as a pass or fail test for new models of cellular telephones. The pass or fail level is the peak SAR value established by the NCRP (National Council of Radiation Protection) Report 86 for the general public exposure, 1.6mW/g [9]. The NCRP 86 exposure limits represented, at the time of the introduction of the portable cellular telephones in 1984, the most stringent US national guidelines for the exposure of humans to RF energy in the frequency band of 800-900 MHz. The 1986 SAR limits of NCRP in the frequency band of cellular communications have been also adopted by the more recent (1992) human safety standard of ANSI (American National Standards Institute), the ANSI C95.1 - 1992. Given the facts that: 1) a specific anatomy is not of great relevance 2) it is important to simulate the maximum coupling of the RF energy between the telephone and the phantom human in normal and unusual conditions of use, one must decide which are the target organs of greatest interest to the effect of peak SAR measurements.

From simple anatomical considerations it is obvious that the cranial skin, the skull bones in the parietal, temporal and occipital regions, the brain mass in the same areas, the acoustic organs

and the lower portion of the face from the ear to the mouth are the regions most exposed to RF energy emitted by the cellular telephone. The posterior portion of the eyes, the tissues of the neck and upper torso and the hand holding the cellular telephone are also exposed to RF energy emanating from the radio.

Let us briefly analyze the significance of the exposure of the organs just listed. The skin, relative dielectric constant  $\epsilon_r = 51$ , conductivity  $\sigma \approx 1.4$  S/m at 800-900 MHz, is a water-rich organ, which readily absorbs RF energy in the cellular telephone band [10], but it is also a very rugged organ constantly exposed to a variety of environmental agents. The same can be said about the hand. The cranial bones are organs from a delicate tissue and their exposure must be carefully considered. Wet bones have lower dielectric constant and conductivity than skin; they have similar dielectric properties to those of the subcutaneous fat that is also present below the skin in the human head. The relative dielectric constant and conductivity of wet bone are  $\epsilon_r \approx 5-6$  and  $\sigma = 70-140$  mS/m, respectively, in the 800-900 MHz band [10].

The dielectric characteristics of live bone tissue have not yet been fully quantified experimentally. This topic will be discussed further in Section 4. The thickness of the bone and subcutaneous fat layer varies between 0.6 and 1 cm over the adult skull with the maximum at the squamous portion (rocca squamosa) of the temporal bone close to the ear

Brain is a tissue also rich in water, but it has also a substantial fatty content, with the exception of the cerebrospinal fluid, which is contained in the ventricles, deep in the cerebral mass. When a portable cellular telephone is in the typical use position, the nearest brain tissue is matter of relatively uniform dielectric characteristics with macroscopic values of dielectric constant and conductivity  $\epsilon_r = 41$  and  $\sigma = 1.1-1.2$  S/m in the frequency band of interest. The eye is another organ of great importance which is proximal to the radio case of cellular telephones. The posterior chamber of the eye is a small globe of tissue rich in water, the vitreous humor with dielectric properties similar to those of skin. The facial region between the ear and the mouth is made up of muscles in addition to the skin and subcutaneous fat. The skeletal muscles involved are the masseter, the zygomaticus major and minor, and the risorius, which form the fleshy strip of facial anatomy between the ear and the mouth. Muscle tissue has a high water content and readily absorbs RF energy in the frequency band of cellular telephones. The dielectric properties of muscle tissue are very similar to those of skin [10].

The tissues in the neck should also be given consideration. In addition to the cervical spine, containing a part of the central nervous system, the main contents of the neck are the muscular masses that move the head, the tongue, the larynx, the pharynx, the trachea, the important thyroid and thymus glands. These organs have very complicated geometries and widely different dielectric properties ranging from air  $\epsilon_r \approx 1$ ,  $\sigma \approx 0$  S/m to skeletal muscle with  $\epsilon_r \approx 51$ ,  $\sigma = 1.4$  S/m in the frequency band of cellular telephones.

The organ closest to the radio case and the base of the antenna is actually the external ear (pinna), where one can reasonably expect the highest values of exposure because of the possible proximity to the strongest RF currents. The external ear is a cartilaginous organ covered by a thin layer of skin, with an appendage, the lobule, made up of essentially fatty tissue. The external ears are rugged organs. They keep the upper part of the radio case and the base of the antenna from direct contact with the skin in the temporal and occipital region of the head.

Given the complexity of the structure of the portion of the human head closest to the cellular telephone, a phantom model could be made to approximate the human anatomy to a sufficient accuracy only with great efforts [11]. The cranial skin and the ears are not easily representable through phantom models. The subcutaneous fat and the skull can be properly modeled by simulated tissue [3]. The same considerations hold for the muscles of the face and the posterior chamber of the eye [12].

Since we are concerned mainly with induction H-fields in materials without magnetic dissipative properties, the deposition of RF energy in bone and fatty tissue near RF currents can be approximated by using simulated brain material in their place. This substitution of phantom tissues, in addition to resulting in a larger simulation of the RF energy absorbed by the organs in the skull beneath the skin, also substantially simplifies the phantom model.

The phantom, used in the RF deposition measurements for cellular telephones, can be a shell of fiberglass about 1.5mm thick, filled with a material simulating brain tissue. Simple and relatively easy to reproduce, it has the significant benefit of giving the worst case SAR absorbed by brain tissue and the skull bones, a necessary feature for safety measurement purposes. It has the disadvantages of not simulating correctly the RF deposition at the surface skin, the earlobes, the facial muscles and the posterior chamber of the eye. As pointed out before, the earlobes and the skin are rugged organs exposed to external physical agents. The facial muscles and the eye, given their greater distance from the

highest RF currents, are not the primary exposed organs of the head, so their accurate simulation, at least in an initial phase, is not as critical as for the brain and the skull. Their exposure can be more accurately simulated with a head phantom having a "cranial" chamber filled with simulated brain tissue and a "facial" chamber filled with simulated muscle tissue. This further refinement of the phantom model will be left for future work, if necessary.

The phantom used in the experimental evaluation of the worst case exposure of the users of cellular telephones is a fiberglass enclosure 1.5mm thick, shaped like a human head, filled with a mixture simulating the dielectric characteristics of brain in the 800-900 MHz band. To maximize the coupling between the simulated user and the telephone, a large model of the human head has been used. The maximum width of the cranial model is 17 cm, the cephalic index is 0.7, and the crown circumference of the cranial model is 61 cm.

The distal part (from the telephone) of the phantom enclosure has been removed from the model so as to permit scanning the probe in the region of the simulated anatomy close to the RF sources. A close-up picture of the phantom model is given in Figure 1.

c. Probe Positioning System and Measurement Instrumentation

In the near field of portable communication antennas in the 800 MHz band, the positioning of the probes must be performed with sufficient accuracy to obtain repeatable measurements in the presence of rapid spatial attenuation phenomena and variations of the field distribution [13]. The smallest physical dimension of the antennas involved in the class of cellular telephones under investigation is of the order of 1mm, so a 0.1mm positioning accuracy in three dimensions is required for SAR measurement repeatability, because the antenna can be arbitrarily close to the target tissue.

The accurate positioning of the E- and H-field sensors has been accomplished by using a robot: the Intelledex MicroSmooth Model 660. The robot can be taught to position the probe sensor following a specific pattern of points. In a first sweep the sensor is positioned as close as possible to the brain surface, with the sensor enclosure touching the inside of the fiberglass shell of the phantom. The SAR is measured on a grid of points 1.0cm apart which covers the curved surface of the head nearest to the portable cellular telephone.

The E-field probes are extremely fragile. To ensure their protection they have been enclosed in a hollow plastic protective

cylinder of 5mm outer diameter and 0.5mm thickness. The external surface of the cylindrical cap protrudes 0.41cm beyond the dipole sensors of the E-field probes. The closest distance that the sensor can be placed to the phantom shell is therefore 0.41cm. The SAR falloff in this 0.41cm gap is estimated by using experimental data, as will be discussed shortly.

Figure 2 shows the robot in a typical measurement session. Figure 3 gives a close-up view of the phantom with the cellular telephone. The position of the cellular telephone is dictated by the human anatomy. The earpiece is located at the ear of the phantom and retained with a Styrofoam fixture, using light holding pressure. If the earpiece cup is located over the inner earlobe for optimum or near optimum sound coupling, the cellular telephone radio case has been shaped to generally follow the human face anatomy and place the microphone by the mouth of the user. The telephone can be tilted away from the face within an angular range of 10-15° without losing the acoustic coupling between the microphone and the mouth (Figure 4A). The telephone position can be altered also by sliding the ear piece over the earlobe or by tilting the radio case so that the microphone is substantially above or below the mouth (Figure 4B). As will be shown later, even substantial perturbations of the telephone position with respect to the one with best acoustic coupling only marginally affect, or actually reduce, the peak SAR in the user's head.

From Figure 3, one can see that the telephone is tested without a hand holding it. The human hand is an anatomical and geometrical complex structure that can assume a practically infinite number of configurations over the radio case. As it will be discussed in the next section, the effect of the hand is generally to reduce the peak SAR in the head. Because of the almost irreproducible SAR effects of the hand over the radio case, it was decided to perform the measurements of the peak SAR in the head without the presence of the hand holding the telephone, thus introducing a bias for higher peak SAR values. This bias for the "worst case" is acceptable in safety measurement.

The origin of the coordinates of the scanning grid is located inside the phantom head at the intersection of the antenna axis and the top surface of the telephone. The coordinate system is oriented so that the positive X axis is in the direction of the antenna and the positive Y axis penetrates the brain mass in the direction of the local normal to the cranial surface; the positive Z axis forms an orthogonal left-handed coordinate system with the positive X and Y axes. These X and Z coordinates are curvilinear and follow the contour of the inside of the phantom cranium. The phantom surface is considered locally planar, at least over a 0.5cm

incremental distance. Figure 5 gives a sketch of the coordinate system used during the measurement sessions.

The coarse scanning on a 1 cm grid locates the region or regions of local SAR maxima at the phantom surface. Since the phantom surface is substantially planar in the sections close to the antenna feed point and the radio case, the peak value of SAR is located at the surface of the simulated tissue mass because of (1) the space attenuation of the magnetic field and (2) the absence of possible lens effects. The latter condition was checked by searching for focusing phenomena in the parietal and occipital regions of the brain, but none was found.

The region or regions of locally maximized SAR are further probed by scanning the surface of the brain over a square grid with 1mm increments. The absolute peak SAR near the surface of the phantom brain is located in this fashion within a square of 2.5mm side. The robot then proceeds with a Y scan (the Y axis penetrates locally the brain mass) at 0.5cm intervals over a 5cm length. A plot of the fall-off of the SAR vs. depth is obtained. From this plot the peak SAR at the surface of the phantom is evaluated using a 3 point interpolation method [14]. In this fashion the SAR falloff in the 0.41cm gap between the sensors and the phantom brain surface is estimated by using experimentally determined attenuation values. The calibration of the probes, described in the next section, shows that no significant experimental error is introduced using this method to evaluate the peak SAR in locally planar phantoms.

A DC electrical signal proportional to the  $|E|^2$  or  $|H|^2$  detected by the sensors forms the input of a DC amplifier designed for this special application. The electronic devices, one channel for each sensor, are contained in a metal box 5.2cm x 4.8cm x 5.8cm, located 30cm from the sensors of the probing devices. The gain of the three amplifiers is variable over the range 10-13 dB and is set once for each channel of the probe, as described in the following section.

The circuitry of the three DC amplifiers has been carefully isolated by metal shielding, so its performance is not affected by the presence of incident electromagnetic fields.

The output of each DC signal amplifier is connected to a voltmeter, one for each channel, by the means of 30 feet of high impedance lines. The DC resistance of this wire is relatively high, 4-5 k  $\Omega$ /ft; the RF resistance is extremely high because the wire is made of carbon composite which is a dielectric at the 800-900 MHz frequency band.



The DC voltage is measured by a millivoltmeter, the HP 3478A, whose output is monitored by a GPIB interface connected to an IBM-compatible PC. A sketch of the electronics is given in Figure 6. The computer is programmed to have the robot move the probes through a predetermined path and perform the electromagnetic field sensing. The probe is driven to the appropriate location, after waiting one (1) sec to let all the mechanical vibrations in the mixture and the robot arm die out, the outputs of the sensors are read by the voltmeters and summed up by the computer. The total voltage is proportional to  $|E|^2$  or  $|H|^2$  depending on the probe used. The typical measurement session for determining the peak SAR of a cellular telephone model takes approximately 20 minutes after the equipment has been set up and the robot has been "trained" to scan over a specific grid.

d. Probe Calibration

The free space calibration of the E-field and H-field probes can be performed using a TEM-cell manufactured by IFI (Instruments for Industry, Farmingdale, New York, 11735) operating at the frequency band of cellular telephones [15] [16]. The SAR calibration of the E-field probe requires a procedure involving temperature increase measurements.

The Vitek Electrothermia Monitor Model 101 was used to determine temperature during the RF exposure of a planar phantom. This thermometer has an RF-transparent sensor system which is nominally non-perturbing to the incident RF field. The temperature increase at the feed point of a balanced dipole operating at 840 MHz was measured at the inner surface of a planar phantom filled with brain-simulating mixture. Figure 7 shows a picture of the planar phantom used in the calibration measurements; note that the probe is positioned by inserting it into the mixture from the free surface side and that the dipole antenna is very close to the surface of the phantom. The initial temperature increase slopes and the relative SAR values for various radiated power levels are plotted in Figure 8. The exposure time of the phantom for each of the points in Figure 8 was 30 secs. The following simple equation relates SAR to the initial temperature slope:

$$\text{SAR } \Delta t = Jc\Delta T \quad (1)$$

In equation (1)  $\Delta t$  is the exposure time (30 seconds),  $J$  is the constant of Joule (1 calorie = 4.185 Joules),  $c$  is the thermal capacity of the simulated tissue ( $c = 0.95$  calories /°C/g) and  $\Delta T$  is the temperature increase due to the RF exposure. Clearly SAR is

proportional to  $\frac{\Delta T}{\Delta t}$  or the initial rate of tissue heating, before

thermal diffusion takes place [17].

From (1) it is possible to quantify the field in tissue using [18]

$$\text{SAR} = \frac{|E|^2 \sigma}{\rho} \quad (2)$$

where  $\sigma$  is the simulated tissue dielectric loss and  $\rho$  its density; in this case  $\rho = 1.25 \text{ g/cm}^3$ .

The E-field probe tip is positioned at the same location as the thermal sensor. Since the E-field sensors are located at 0.41cm distance from the surface of the phantom, this field attenuation in the corresponding tissue layer is computed in the following fashion. The probe is scanned along the normal to the plane phantom at the point of thermal measurement. A plot of the field attenuation is obtained, as in Figure 9, where it is also shown the result of the extrapolation method used to compute the  $|E|^2$  field at the surface of the phantom, where there is the maximum SAR. This method has given highly repeatable results. The linearity of the incremental temperature readings of the VITEK thermometer is excellent, as checked with a thermocouple standard. The experimental error in the determination of the SAR using the E-field probe method is less than 10%, if a transmitter with more than 5W radiated is used in determining the temperature increase during a 30 second exposure.

### III. Experimental Results

All measurements reported in this section have been performed with 0.6W RF (maximum setting) power output from the cellular telephones tested.

#### a. Tested Telephone Models

There are two classes of portable cellular telephones, which have been evaluated in terms of the SAR exposure of the user. The first class has been commercially available since 1984. These telephones, since they are derivatives of the old model, are called Dynatac™ or "classic". A typical sample of the classic telephones is shown in Figure 10. The classic telephones have a case dimension (front-to-back distance) varying between 6.0cm and 8.0cm. All these telephones have a shortened sleeve dipole 14cm long (shown in Figure 10).

The other type of cellular portable devices has been commercially available since 1989. These are called Micro TAC™ personal telephones also known as "flip" telephones. The flip telephone radio case (without the battery), depending on the model, has a dimension (front-to-back distance) varying between 2.5cm and

2.0cm, the most recent models being the thinnest. All flip telephone models have a two hour (2h) battery, 1cm thick, and an 8h battery, 2cm thick. The type of battery has practically little effect on the SAR measurement results.

The flip telephones have a dual antenna system. Please refer to Figure 11, where the same telephone is shown with its antenna extended and collapsed. In the dome above the telephone case there is a small 1.75cm long helical wire, which forms the RF radiator with the metal in the radio case, when the primary antenna is collapsed. The primary antenna is a half wave dipole, 12cm long, end fed by the helical wire, when pulled out of the radio case [19]. Typical free space magnetic field measurement results for the flip telephones are shown in Figure 12 (antenna collapsed) and Figure 13 (antenna extended). The free field patterns have been recorded by moving the sensor at a constant 5mm distance from the radio case and the antenna. The salient features of the patterns in Figures 12 and 13 are the peaks of the H-field at the feed point of the helical wire and the substantial decrease of the H-field intensity over the radio case, when the primary antenna is extended.

Figure 14 shows the results of the  $|H|^2$  field measurements recorded by moving the H-probe at 5mm distance from the radio case and the antenna of a typical classic cellular telephone. It is worth noting that the center-fed sleeve dipole does effectively choke the RF current on the radio case, which is not an integral part of the radiating mechanism as in the case of the flip telephone. This is rigorously true only in the free space conditions.

#### b. Results of the SAR Measurements

Dozens of portable cellular telephones have been tested since the introduction of these devices in 1984. The results are best summarized in tabular form, as in Table 1 and 2. The tested telephone models are kept in an archive and are retested whenever any component of the SAR measurement system is upgraded or modified. All new portable telephone models are tested for compliance with the SAR limits of NCRP-86 as part of the new model shipping acceptance.

Table 1 gives the maximum and the minimum values of measured SAR averaged over 1g of tissue for the "classic" portable telephones.

The columns of Table 1 refer to various services that are offered in cellular telephony in the United States and in Europe. FMCW identifies the Frequency Modulation of the RF Continuous Wave

almost universally used at the present time (August 1993) by cellular telephones. GSM (Groupe Systemes Mobiles) is the new digital service of the Pan-European cellular mobile telephones; the RF signal of the subscriber unit is pulsed at 217Hz, each channel can service 8 users. The average RF power driving the pulse is 2W, the time average is 0.25W. The NADC (North American Digital Cellular or IS 54) is a multiple-access cellular service, three users to a channel; the subscriber unit transmits an RF signal pulsed at 50Hz. The average RF power during the pulse is 0.6W, the time average being 0.2W. The NADC service has been introduced in 1993.

Table 2 compiles the measured peak SAR values for the flip telephones. The data in Tables 1 and 2 have been collected without a human hand holding the telephone.

As one can see, there is substantial dispersion of the experimental SAR values within each telephone model of the various transmission strategies. The dispersion is due to various positions of the radio case, to different sizes of the radio case and to different packaging of the electronic subassemblies within the radio case.

It is essential, at this point, to locate the position of the peak SAR values within the phantom. The worst case map of the measured SAR values at 0.41 cm inside the simulated tissue, using a FMCW flip telephone with collapsed and extended antenna, is shown in Figures 15A and 15B, respectively. Although the peak SAR values in Figure 15A exceed 1.6 mW/g, the one gram average of SAR is 1.6 mW/g or less. Figure 15C shows a similar map for the classic phones. The values given in Figures 15A-C are the detected SAR levels without averaging them over 1g of tissue shaped like a cube.

Figure 16 plots the SAR pattern at the surface of the simulated brain tissue in the plane parallel to the antenna axis and containing the point of peak SAR. In Figure 16 is also shown an outline of the phantom contour. The origin of the X axis is the bottom of the touch-tone pad; the X axis which follows the inward surface of the human head has been rectified for ease of representation. Note that the peak SAR is in the temporal area of the phantom user. Analogous information is shown in Figure 17 for a GSM "classic" portable cellular phone.

**TABLE 1****Measured Peak SAR Values from "Classic"  
Portable Cellular Telephones**

ANTENNA	FM CW	GSM (2W)	NADC (0.6W)
Dipole	0.2 - 0.4	0.09 - 0.1	0.07 - 0.09

All SAR values are in W/kg averaged over 1g of tissue shaped like a cube. For the GSM and NADC telephones the peak SAR value is also time-averaged over the frame of the signal. The range of values is due to different models and operating positions. No hand holds the phones.

**TABLE 2****Measured Peak SAR Values from "Flip"  
Portable Cellular Telephones**

ANTENNA	FM CW	GSM (2W)	NADC (0.6W)
Collapsed	0.9 - 1.6	0.2 - 0.3	0.2 - 0.8
Extended	0.6 - 0.8	0.1 - 0.2	0.1 - 0.4

All SAR values are in W/kg averaged over 1g of tissue shaped like a cube. For the GSM and NADC telephones the peak SAR value is also time-averaged over the frame of the signal. The range of values is due to different models and operating positions. No hand holds the phones.

From the results shown in Figures 16 and 17 one can see that the exposure of the face of the phantom is well diffused over the entire area of the radio case and the base of the antenna. The exposure values are peaked at essentially very few locations, one or two.

Figure 18 shows the region of the human head where the peak SAR values have been detected for all the portable telephones tested using the phantom described in Section II b. Note that no SAR peak was found past the earlobe in the temporal area. Most peak SAR's are detected in the area of the display and of the touch-tone pad, located just below the plastic case of the telephone, which is touching the face of the phantom in the area close to the ear. The antenna, except for its feed point at the top of the telephone case, causes no sharp SAR peaks in the occipital or parietal area of the head.

The effects of a hand holding the telephone have been difficult to quantify reliably. The results of the experiments are briefly summarized, because of their lack of repeatability. If the radio case is lightly held by the finger tips, practically no effect on its SAR patterns and their peaks have been detected. In general, the SAR patterns of the "classic" telephones are affected minimally by the location or the position of the palm of the holding hand. "Flip" telephone SAR performance is affected by the touch of the palm of the hand over the radio case and its location. Measurements show that peak SAR values are 10-30% lower if the palm of the hand is in direct contact with the radio case, the higher value is detected if the hand is close to or on top of the base of the antenna.

#### c. Antenna Shields

Two types of antenna shields have been tested. One is called Cell Shield manufactured by Dynaspek Inc. [20]. The device is a hemicylinder 15cm long, with a radius of 2cm. Its base makes electrical contact with the ground of the antenna. The device fits only the "classic" type of cellular telephones. Installed following the directions supplied, the shield is placed between the antenna and the head of the user.

The other device, called Cell-u-Shield, manufactured by Cellu-Shield of Palm Beach, Florida, also fitting only the "classic" telephones, is a metal wedge about 15 cm long, 2cm wide on the side which must be shrink-wrapped around the antenna. The metal wedge also must be located between the head and the antenna; this device does not contact the antenna ground and is electrically floating. Both devices perform an electromagnetic shielding function at a substantial cost to the gain of the antenna. Table 3 shows the results of the SAR and gain measurements

performed using various models of the "classic" telephones with and without the two shields.

TABLE 3		
Antenna Shields Performance		
Parameter	With/Without Cell Shield	With/Without Cell-u-Shield
Average Gain (dBi)	-12.5 / -1.1	-11.7 / -1.1
Peak SAR Value (W/Kg)	0.008 / 0.38	0.06 / 0.38

The peak SAR value measurements have been performed following the methods described in Section II of this paper. The average gain was measured by integrating the contour plots of the radiation patterns taken over an angular section 360° in azimuth and  $\pm 18^\circ$  in elevation.

Both devices shield the users not by redirecting the RF energy in space as claimed in [20] but by reflecting it back into the telephone where it is dissipated in the filter and the heat sink of the final RF amplifier of the radio. During the tests the telephone RF amplifiers become extremely hot, beyond their normal temperature range. There are two serious disadvantages for the users of these shields. One is the obvious loss of coverage. With a gain loss of about 11 dB, the user can expect a drop in range of a factor of 2 to 3 in an urban environment [21], and a consequent loss of area coverage by a factor of 4 to 9. In these conditions, on average, the telephone can be used to carry on a conversation only 25% to 10% of the time compared to full coverage. The other big disadvantage is that the RF power output of the telephone transmitter will be kept nearly always at the maximum level because of low signal strength at the base station [22], thus causing overheating and loss of useful life of the telephone.

Another type of device that purports to protect the user of portable cellular telephones from absorbing RF energy is the Ireland Antenna. This antenna is marketed by Universion Systems Inc. of Miami, Florida and fits only the "classic" type of telephones. The literature of this product states: "The unique technology in the reactance cancellator eliminates the ground return system, which means that the human body does not absorb the radiation from the antenna."

The Ireland antenna is a half-wave whip base-loaded with a matching coil. This type of radiating element is analogous to the "long" antenna offered with the "classic" telephones. Figure 19 plots the near H-field values recorded at 0.5 cm distance from the "classic" telephone with the antenna shipped by the manufacturer, while Figure 20 shows the same results using the Ireland Antenna.

As one can see, the RF currents on the radio case side which is placed against the head of the user are no different for the two antennas.

#### IV. Comments

The experimental results given in Section III clearly refer to no human. The phantom is a control model, not a real model. Yet the SAR values shown in the previous section can be interpreted to provide the range of the highest expected values of the exposure of the brain of humans using cellular telephones. Although fatty tissues do not absorb RF strongly because of their hydrophobic properties, living bones are perfused by fluids rich in water and cellular nutrients, which cause the relative dielectric and the RF attenuation constant to be not much lower than those of brain tissue. In various attempts to treat brain tumors by RF diathermy, it was found that it was very difficult to heat the brain tissue of anesthetized animals (particularly swine) at 915 MHz because of the RF absorption of the bones of their head [23]. Although reliable data are not available for the electrical characteristics of living bone in the 800-900 MHz frequency band, it is reasonable to use for the following considerations the dissipation factor of brain tissue in characterizing the RF attenuation in the skull bones adjacent to the cellular telephone as shown in Figure 18. Recent measurements show that this hypothesis is essentially correct [24].

Using the space attenuation and the RF dissipation factor of simulated brain tissue in assessing the field decrease in the bones, in the surface skin and the subcutaneous fat of the temple, which are 0.7 - 1cm thick, one can see from Figure 9 that the exposure at 0.7 - 1cm inside the simulated tissue is attenuated by about a factor of 1.6 with respect to the peak value, which is always at the surface of the planar model. If we apply the same attenuation factor of 1.6 to the SAR values in Tables 1 and 2, one finds that the FMCW cellular telephones expose brain tissue to localized peak SAR values in the range 0.1 - 1.0 W/kg. At these levels the exposure can be considered athermal, that is causing no macroscopic temperature increase above the physiological range of the target tissue.

Brain tissue is metabolically very active. The brain absorbs approximately one fifth to one sixth of the blood flow output of the heart [25]; the basal metabolic rate of human brain tissue is in the range of 8 -



10 W/kg, that is a full order of magnitude higher than the peak localized SAR of the exposure. In addition, the peak exposure of the brain is always at the surface of the organ, where are the pia mater and the outer cerebral cortex. The pia mater is a vascular membrane covering the surface of the cerebral cortex as a rich capillary bed; the outer cerebral cortex is also rich in capillaries.

The local anatomy and physiology of the brain exposed to the highest values of electromagnetic energy absorption rate in simulated brain tissue from portable cellular telephones tend to exclude the possibility of a macrothermal exposure of the human brain.

Microthermal effects, of the type discussed in [26], cannot be excluded at this time, given the gross characteristics of the phantom and the probes used in this study. However, a runaway temperature increase in brain tissue at the microscopic level is difficult to conceive at the exposure levels presented herein. At the present time there are neither scientific evidence nor credible theoretical models of the interaction between EM fields and living tissue that indicate an adverse biological effect at athermal levels of exposure to constant amplitude 800 - 900 MHz waves with incoherent phase [27 - 28]. These are the characteristics of the FM signals emitted by cellular telephones.

## V. Conclusion

A practical method and control model to evaluate the RF exposure of humans using portable cellular telephones have been presented. The model tends to overstate the exposure of cerebral tissue as compared to more realistic anatomical models.

Although the model and RF sensors can indicate only the gross features of the RF absorption by the telephone users, the results collected so far suggest that adverse biological effects from thermal damage are highly unlikely or outright impossible. Given the physical characteristics of the RF waves used in analog cellular telephony (FM) there are no other known mechanisms of adverse bioeffects that can be attributed to the cellular telephone usage on the basis of existing scientific knowledge.

Future work will endeavor to refine both the anatomical model and reduce the size of the RF sensors, so that microthermal effects (if any) at tissue boundaries can be experimentally detected. At this time there is a considerable theoretical effort to predict the exposure of a user of cellular telephones by computer simulation [29]. This theoretical effort will facilitate future experimental investigations using more realistic phantoms. The results given in [29] show SAR levels lower than those reported herein. The reader should not be surprised because the model presented in this paper gives an upper bound of the exposure of the users of cellular telephones.

Although research to date suggests that pulsed RF signals such as those of GSM and NADC, which are below or substantially below the NCRP protection guidelines, are also biologically neutral, the data do not yet permit so ready a conclusion to that effect as is the case for FM signals. Biological research should and is being conducted to test further the hypothesis that the new cellular telephone RF signals are as biologically neutral as are the FM systems they are replacing.

#### Acknowledgment

The authors wish to thank Dr. W. Ross Adey, M.D., of the Loma Linda Medical Center, Loma Linda, California, for many years of guidance in the area of the biological effects of RF electromagnetic fields and Mr. Howard Bassen of the Food and Drug Administration, Center for Devices and Radiological Health, Rockville, Maryland, for his contribution to experimental RF dosimetry.

Also the accurate typing of Ms. Kaye DeMuro is gratefully acknowledged.

## References

- [1] M. Fischetti, "The Cellular Phone Scare" IEEE Spectrum June 1993, pg. 43-47.
- [2] N. Kuster and Q. Balzano, "Energy Absorption Mechanism by Biological Bodies in the Near Field of Dipole Antennas above 300 MHz" IEEE Transactions on Vehicular Technology Vol. 41, No. 1, Feb. 1992, pg. 17-23
- [3] Q. Balzano et al., "Energy Deposition in Simulated Human Operators of 800 MHz Portable Transmitters". IEEE Transactions on Vehicular Technology, Vol. VT-27, No. 4, Nov. 1978, pg. 174-181
- [4] R. Pethig "Dielectric and Electronic Properties of Biological Materials" John Wiley and Sons, Lt., 1979, Chapters 1 and 2.
- [5] J. L. Kirschink et al. (1992) "Magnetite Biomineralization in the Human Brain" Proc. Nat. Acad. of Science (in press).
- [6] H. Bassen "Internal Dosimetry and External Microwave Field Measurements Using Miniature Electric Field Probes" Proceeding of the Conference on Biological Effects and Measurements of Radio Frequency/Microwave, Rockville, MD Feb. 16-18, 1977, pg. 136-151.
- [7] Q. Balzano and K. Siwiak "The Near Field of Annular Antennas" IEEE Transactions on Vehicular Technology Vol. VT-36, No. 4, Nov. 1987, pg. 173-183.
- [8] A. W. Guy and C. K. Chou "Specific Absorption Rate of Energy in Man Models Exposed to Cellular UHF Mobile Antenna Fields" IEEE Trans. on Microwave Theory and Techniques, Vol. MTT-34, No. 6, June 1986, pg. 671-680.
- [9] NCRP Report No. 86 National Council on Radiation Protection and Measurements, 7910 Woodmont Av., Bethesda, MD. 10814, pg. 284
- [10] C. C. Johnson and A. W. Guy "Nonionizing Electromagnetic Wave Effects in Biological Materials and Systems" Proceeding of IEEE Vol. 60, June 1972, pg. 692-718.
- [11] G. Hartsgrove et el "Simulated Biological Materials for Electromagnetic Radiation Absorption Studies" Bioelectromagnetics, Vol. 8, No. 1 , 1987, pg. 29-36.
- [12] R. F. Cleveland and T. W. Athey "Specific Absorption Rate (SAR) in Models of the Human Head Exposed to Hand-Held UHF Potable Radios" Bioelectromagnetics, Vol. 10, No. 2. 1989, pg. 173-186.

- [13] Q. Balzano et al "The Near Field of Omnidirectional Helical Antennas" IEEE Transactions on Vehicular Technology, Volt. VT-31, No. 4, Nov. 1982, pg. 173-185.
- [14] "Handbook of Mathematical Functions" Edited by M. Abramowitz and I. Stegun, Dover Publications, May 1968, Section 25, pg. 877-878.
- [15] M. L. Crawford "Generation of Standard EM Fields Using TEM Transmission Cells" IEEE Transactions on Electromagnetic Compatibility, EMC-10, Vol. 4, Nov. 1974, pg. 189-195.
- [16] ANSI C95.3 -1991 Recommended Practice for the Measurement of Potentially Hazardous Electromagnetic Fields - RF and Microwaves, Section 4.5.3.
- [17] C. C. Johnson and A. W. Guy "Nonionizing Electromagnetic Wave Effects in Biological Materials and Systems" Proceeding of IEEE Vol. 60, June 1972, pg. 702.
- [18] Ibidem
- [19] Q. Balzano "Land Mobile Antenna Systems" J. James and K. Fujimoto editors. Chapter 4, Section 1.1.2 Artech House. In print.
- [20] Mobile Products News, June 1993, Vol. IX, Number 6, pg. 53-54.
- [21] G. D. Olt and A. Plitkins, "Urban Path-Loss Characteristics at 820 MHz" IEEE Transactions on Vehicular Technology, Vol. VT-27, No. 4, Nov. 78, pg. 189-197.
- [22] CTIA, FDA Presentation, February 19, 1993. "Primer on Cellular Operations".
- [23] Dr. C. Sutton, Private Communication, November, 1979.
- [24] Dr. Camelia Gabriel, University Microwave, London, U.K. Private Communication, September 1993.
- [25] A. C. Guiton "Text Book of Medical Physiology" Fifth Edition, WB Saunders Co., 1976, Chapter 20, pg. 251, Table 20-1.
- [26] W. R. Adey "Tissue Interactions with Nonionizing Electromagnetic Fields " Physiol. Rev. (1981) 61:435-514.
- [27] K. H. Illinger "Spectroscopic Properties of in vivo Biological Systems" Bioelectromagnetics Volume 3, No. 1, 1982, pg. 9-16.

- [28] W. R. Adey "Mechanism Mediating Athermal Bioeffects of Nonionizing Electromagnetic Fields" Invited Paper, 1993 National URSI Conf., Kleinheubach, Germany.
- [29] O. Gandhi "Electromagnetic Absorption in the Human Head and Neck for Some Cellular Telephones" Private communication, December 2, 1993.

## FIGURE TITLES

Figure 1	Phantom Model
Figure 2	Robotic Positioning System
Figure 3	Phantom with Cellular Phone
Figure 4A	Cellular Phone Tilted Away from the Face
Figure 4B	Cellular Phone Positioned Below the Mouth
Figure 5	Phantom Coordinate System
Figure 6	Computer Based Data Collection System
Figure 7	Planar Phantom Used for Calibration of Instruments
Figure 8	Initial Temperature Increase and SAR Calibration Curves
Figure 9	Field Attenuation vs. Depth
Figure 10	"Classic" Cellular Phone Model
Figure 11	"Flip" Cellular Phone Model
Figure 12	H-Field Scan (Antenna Collapsed) of "Flip" Phone
Figure 13	H-Field Scan (Antenna Extended) of "Flip" Phone
Figure 14	H-Field Scan of "Classic" Phone
Figure 15A	SAR Map Flip Phone with Collapsed Antenna
Figure 15B	SAR Map Flip Phone with Extended Antenna
Figure 15C	SAR Map Classic Phone
Figure 16	Plot of Peak SAR Distribution Flip Phone Antenna Collapsed
Figure 17	Plot of Peak SAR Distribution GSM Cellular Phone
Figure 18	Area of Detected Peak SARs
Figure 19	H-Field Scan Classic Phone with Standard Antenna
Figure 20	H-Field Scan Classic Phone with Ireland Antenna



Figure 1 Phantom Model

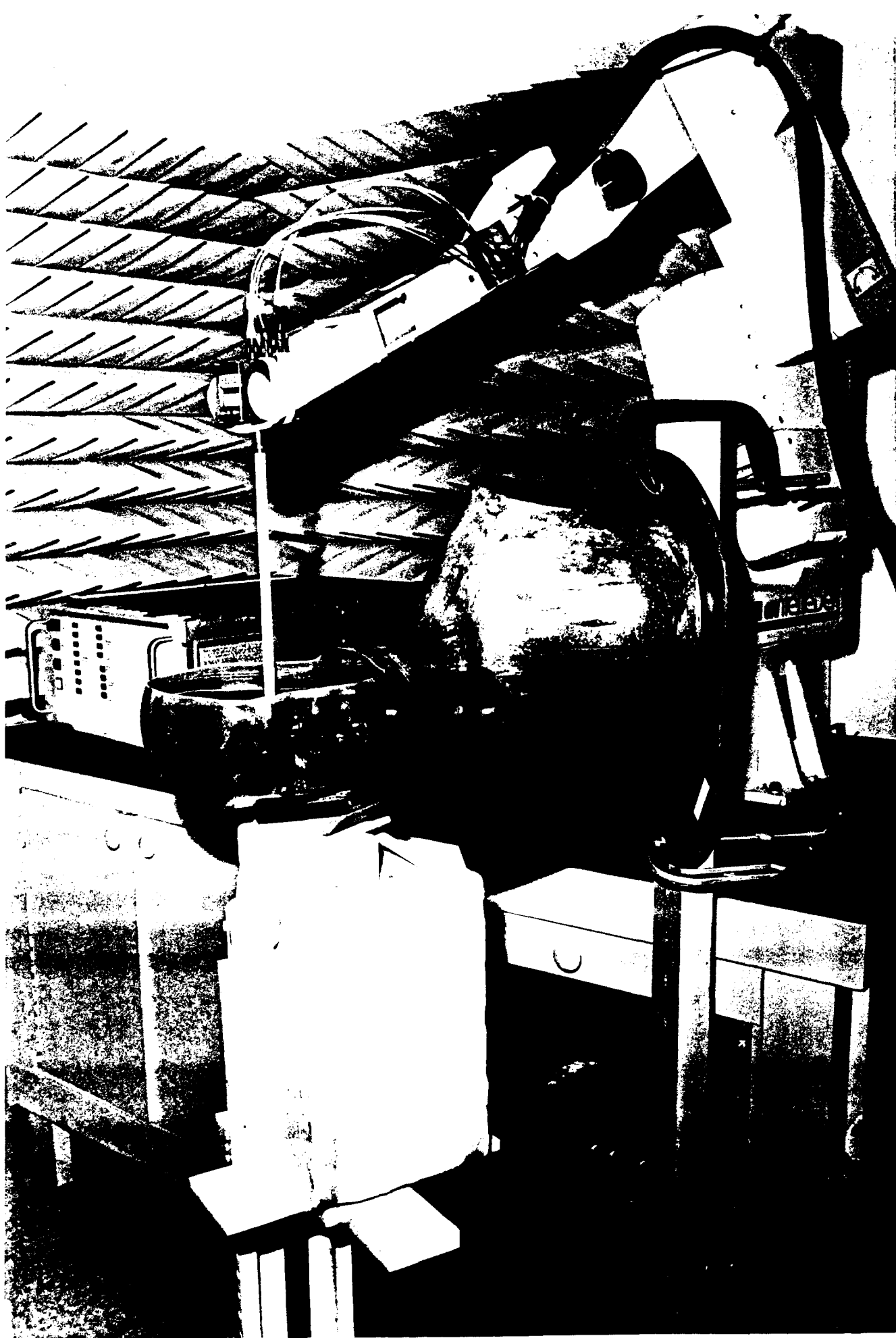


Figure 2      Robotic Positioning System





Figure 3 Phantom with Cellular Phone